Mapping the Milky Way with the 21-cm Hydrogen Emission Line

By
Will Miller
Department of Physics
Allegheny College
Meadville, Pennsylvania

April 27, 2023

Submitted in fulfillment of the senior thesis requirements of the
Department of Physics at Allegheny College
and approved by the senior thesis committee.

Dr. Willey	**Date**	**Dr. Poynor**	**Date**

Pledge

Mapping the Milky Way with the 21-cm Hydrogen Emission Line

By

Will Miller

Department of Physics

Allegheny College

Meadville, Pennsylvania

April 27, 2023

Acknowledgements

First and foremost: I'd like to thank Dr Willey for being my advisor for this comp, helping me get started with this amazing project, and offering advice when I got stuck.

To Dr Lombardi: Thank you for being my advisor for the past 4 years, helping me through the trials of scheduling college courses, and for originally showing me everything the physics department had to offer back in 2018.

To my friends and acquaintances: Thank you for everything, all the good and weird times we had together. Nate and Luke, thanks for being there since the beginning, you guys are brilliant. Same for my current roommates, thanks for four years of memories. To the many people in ARGO and LAG, I couldn't have asked for a more fantastic group to spend my time with. I never expected I'd live through a history-defining pandemic with all of you.

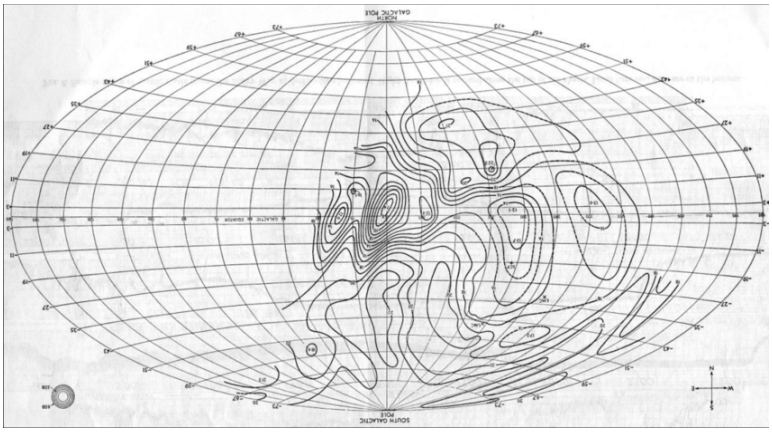
To my roommates: Mike, Joel, and Sam, thanks for the fun times in various clubs, and the bonding moments we had together when we realized that we were all struggling with our comps.

To my Mom, Dad, and Andrew: Thank you for always being there to support me. I know this wasn't an easy major for me and I struggled a lot, but you were always there.

History

History of Radio Astronomy

Radio astronomy has been an important field of study since its creation in the 1930's. In 1932, Karl Jansky, an engineer at Bell Laboratories, discovered a constant source of static when looking at short-wave radio transatlantic communications [1]. After tracking it with the movement of the sky over many months, he discovered that the source of it was in the center of the Milky Way galaxy, in the constellation Sagittarius. Jansky writes "I have taken more data which indicated definitely that the stuff, whatever it is, comes from something not only extraterrestrial, but from outside the solar system. It comes from a direction that is fixed in space and the surprising thing is that …[it] is in the direction towards which the solar system is moving in space. According to Skellett [the astronomer he consulted for help]…there are clouds of "cosmic dust" in that direction…" [1]. Jansky's discovery motivated a radio engineer named Grote Reber to try and work with Jansky on radio waves. Because he wasn't able to get hired by Bell Labs, he built his own parabolic telescope in his backyard. After observing for a year at three frequencies (3300 MHz, 900 MHz, 160 MHz), he found galactic radio waves. He presented his data as contour maps, the Milky Way indicated as the bright areas, as seen below [2].



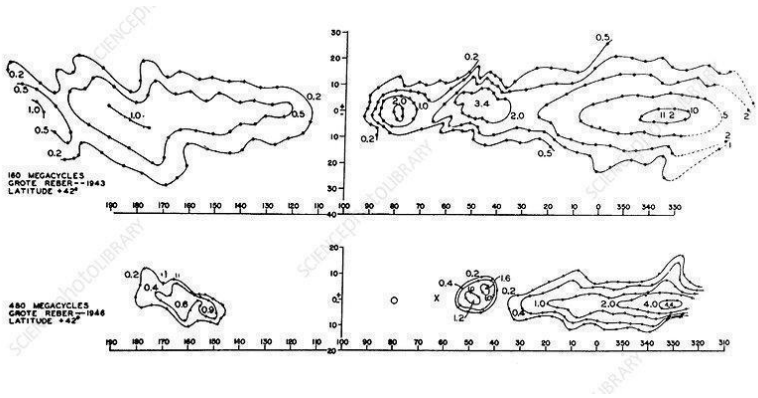


Figure 1.1 [2]: Radio map of the Milky Way made by Grote Reber in 1944.

Another important part of the history of radio astronomy was the suggestion put forward by H. C. van de Hulst. He postulated that the 21 cm emission line, thought at the time to be emitted by neutral hydrogen clouds in the plane of the galaxy, could be detected in interstellar space in 1945. However, their team's receiver was destroyed in a fire, so the suggestion was first verified with the discovery of the interstellar emission by Ewen and Purcell at Harvard University, who informed Hulst's team so they could make multiple successful discoveries before publication [3]. The explanation for why neutral hydrogen clouds emit the 21-cm line is explained on page 9.

The Carr Hall Radio Telescope and previous Comp work

The telescope currently in the Carr Hall garden is critical to this comp. a parabolic reflecting telescope, which means it collects the incoming radio waves as they bounce off the dish into a specified area for data collection. The radio waves are collected in the feedhorn (seen in Figure 1.2) at the center of the telescope dish, before going through the Low-Noise Amplifier, which amplifies the signal 100-fold so it shows up on the graphs. It's then sent through an RF (Radio Frequency) cable to a backend that amplifies the frequency again and converts it to DC voltage, before being sent to the computer which analyzes the data. The data setup is explained in the Methodology section. The computer setup is simple, it's a Windows 10 operating system, with the controls for moving the telescope attached. There are four applications that are

important for this project: PstRotator, which controls the azimuth and altitude movement of the telescope, SpectraCyber II, which graphs the collected data, VirtualBox, which runs a Windows Vista emulator that SpectraCyber II needs to run on, and Stellarium, to get the correct galactic longitude and latitude to position the telescope toward. The uses of these programs will be expanded upon in the Methodology section.

While the telescope itself and the other systems are running fine today, a lot of work had to be done in previous years by Austin Shaw and Ben Ramsey to make sure of that. Austin initially repaired the telescope during his senior year in 2018, and Ben was tasked with bringing the telescope back online in 2019. Ben ran into problems such as the altitude motor shorting out and needing to be replaced, which led to the summer and early autumn being spent fixing/ replacing it.

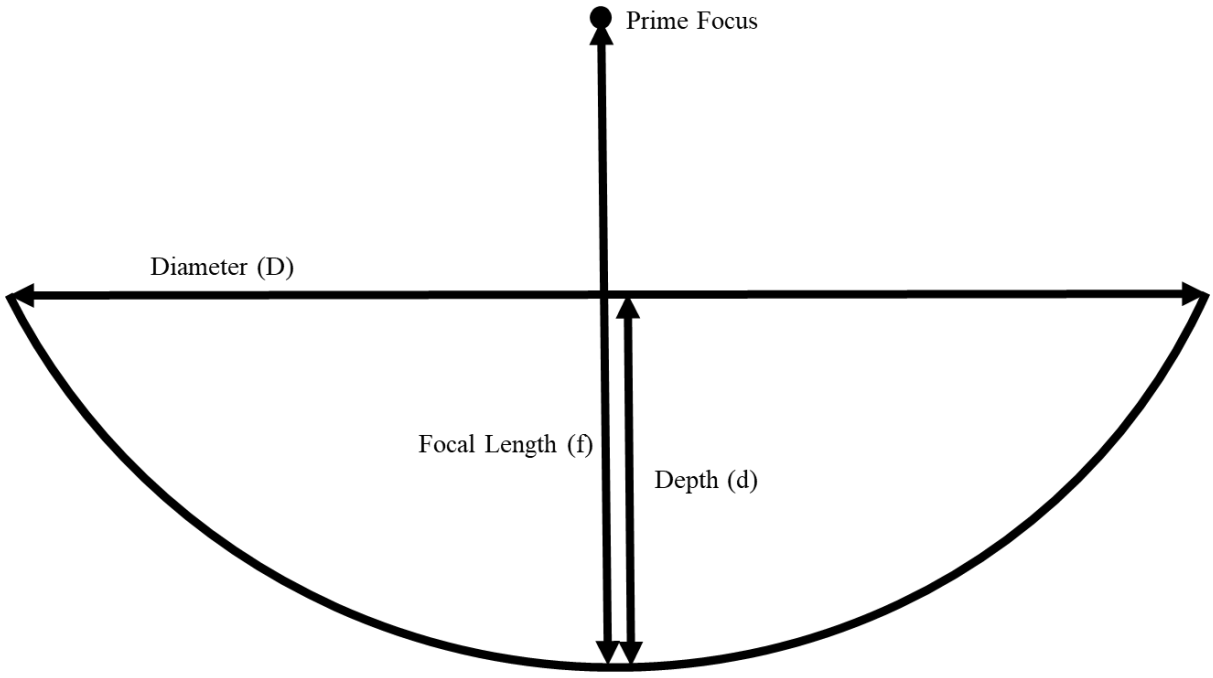


Figure 1.2 [12]: A diagram of a parabolic reflecting telescope. The prime focus is where the feedhorn is located.



Figure 1.3: A photo of the Carr Hall radio telescope



Figure 1.4: A zoomed-in photo of the telescope feedhorn. The small box attached to the black and blue cables is the Low Noise Amplifier.

Theory

Electromagnetic Theory

Before we get into the tricky quantum mechanics involved in the 21-cm hydrogen emission line, we need to start with the nature of electromagnetic waves, arguably the reason this project exists.

In 1873, James Clerk Maxwell created the theory of electromagnetism by bringing together all known laws of electricity and magnetism, which unified the forces that were previously thought of as separate waves. The combined waves are orthogonal to each other, with the magnetic field B propagating along the x-axis and the electric field E propagating along the y-axis, as seen in Figure 1.5 below. The magnitude and direction of both components are given by the Poynting Vector:

$$S = \frac{1}{\mu_0} E \times B \qquad (1.01)$$

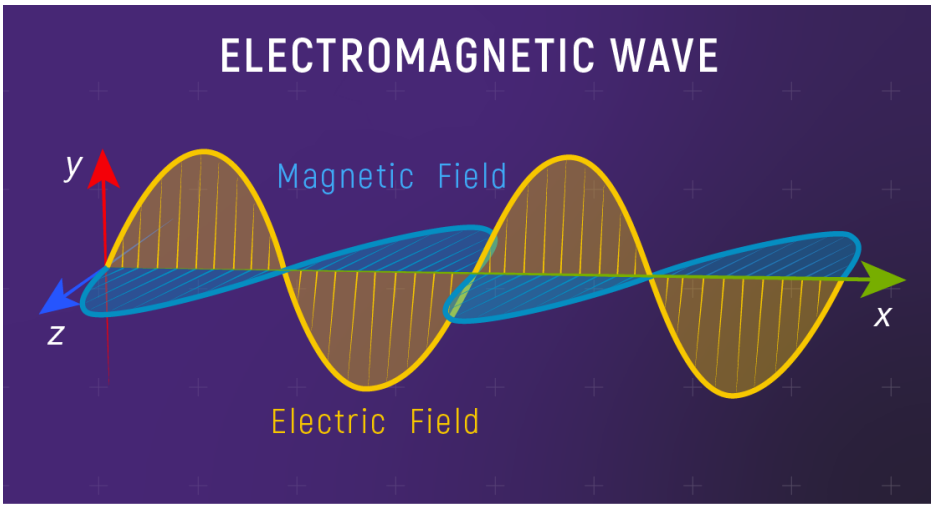


Figure 2.1 [10]: A diagram of the Electromagnetic Wave, showing the Magnetic Field B perpendicular to the Magnetic Field M.

This theory was proven in 1887 by Heinrich Hertz when he created the spark-gap transmitter. The generator creates a pulse of current in the gap between the antenna, and the electric field travels outward at the speed of light, which propagates and creates a wave. The wave carries a magnetic field as well, which is seen when the electromagnetic wave disturbs the surrounding electric field. The disturbed field moves the charges in a loop, creating a current. This generates enough voltage to create a spark, which shows that an electromagnetic wave was created [4]. A diagram of the wave's movement in relation to the generator is shown below.

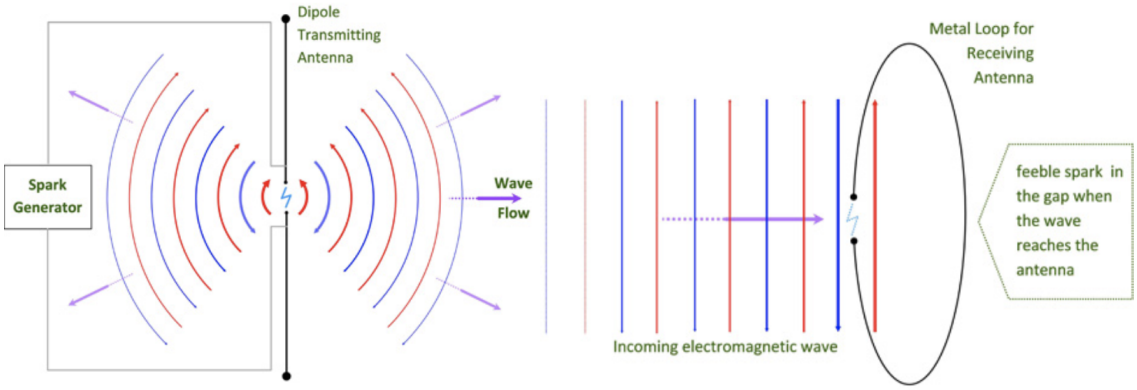


Figure 2.2 [4]: Propagation of electromagnetic waves in a spark-gap generator.

Electromagnetic Spectrum

Visible light isn't the only type of electromagnetic radiation in the universe. In 1800, William Herschel discovered infrared light when he was measuring the temperature in an area where light was refracted through a prism. He measured an increase in temperature beyond red light. On the other side of the visible light spectrum, Johann Ritter discovered ultraviolet light in 1801 when he found that invisible rays just past the violet part of the visible light spectrum darkened chloride-soaked paper faster than violet light. They were originally called chemical rays, as opposed to the old term for infrared, which was heat rays. Heinrich Hertz was the first to intentionally create previously unobserved electromagnetic radiation with his spark-gap generator when he created radio waves with a wavelength of 4 meters [5]. Now, these wavelengths (and many more) are organized on a scale called the electromagnetic spectrum, which is shown in the figure below.

Class			Wave-length λ	Freq-uency f	Energy per photon E
Ionizing radiation	γ	Gamma rays	1 pm	300 EHz	1.24 MeV
	HX	Hard X-rays	10 pm	30 EHz	124 keV
	SX	Soft X-rays	100 pm	3 EHz	12.4 keV
			1 nm	300 PHz	1.24 keV
	EUV	Extreme ultraviolet	10 nm	30 PHz	124 eV
	NUV	Near ultraviolet, visible	100 nm	3 PHz	12.4 eV
			1 μm	300 THz	1.24 eV
	NIR	Near infrared	10 μm	30 THz	124 meV
	MIR	Mid infrared	100 μm	3 THz	12.4 meV
	FIR	Far infrared	1 mm	300 GHz	1.24 meV
Micro-waves	EHF	Extremely high frequency	1 cm	30 GHz	124 μeV
	SHF	Super high frequency	1 dm	3 GHz	12.4 μeV
	UHF	Ultra high frequency	1 m	300 MHz	1.24 μeV
Radio waves	VHF	Very high frequency	10 m	30 MHz	124 neV
	HF	High frequency	100 m	3 MHz	12.4 neV
	MF	Medium frequency	1 km	300 kHz	1.24 neV
	LF	Low frequency	10 km	30 kHz	124 peV
	VLF	Very low frequency	100 km	3 kHz	12.4 peV
	ULF	Ultra low frequency	1 Mm	300 Hz	1.24 peV
	SLF	Super low frequency	10 Mm	30 Hz	124 feV
	ELF	Extremely low frequency	100 Mm	3 Hz	12.4 feV

Figure 2.3 [13]: The Electromagnetic spectrum, with corresponding wavelengths and frequencies.

Radio waves are the largest wavelength that we know of. Due to their low frequencies, they are able to pass through the atmosphere and interstellar dust clouds unobstructed, which is useful for many reasons. It means that radio telescopes can be located on the ground instead of in

space, as atmospheric disturbance isn't a factor. It also means that the hydrogen emissions, which are radio waves at a frequency of 1420.4 MHz, can pass through the interstellar clouds of dust and gas in the plane of the galaxy. This allows us to receive these signals without issue, and to use these signals to map out regions of the galaxy that would normally be obscured by visible light.

Chemical Composition of the Interstellar Medium

Around 75% of the galaxy is made up of Hydrogen, in the form of gas clouds throughout the plane of the Milky Way. As mentioned earlier, these clouds block visible light from the stars within the galaxy and extragalactic objects in that direction. This area is called the Zone of Avoidance, as astronomers can't observe objects in the region. However, radio waves can see through the Hydrogen, thus allowing observations of places such as the supermassive black hole Sagittarius A* at the center of the galaxy.

The Spin-Flip Transition and Hyperfine Splitting

The reason neutral hydrogen (HI) emits along the 21-cm line at 1420.4 Mhz is due to a quantum mechanical phenomenon known as the spin-flip transition. The spin-flip transition can only occur in neutral hydrogen, which has one proton and one electron. These particles aren't spinning in the classical sense, spin, in this case, refers to their intrinsic angular momentum. There are two spin states a particle can have, either positive or negative. A particle with spin and a charge has a magnetic field, so both the proton and electron are magnetic dipoles that interact with each other. If their spins are parallel (both positive or negative), the energy is higher than when they're antiparallel [6]. The result of the difference in energy is known as hyperfine splitting. To get the specific values of a 21 cm wavelength and 1420.4 MHz frequency, we have to use a first-order perturbation. The steps for how to do so and laid out by David Griffiths in his 1982 paper [6]. We start with the potential energy of a magnetic dipole, but with the hamiltonian:

$$H = -m \bullet b \qquad (1.01)$$

Now we also need the formula for the energy of one magnetic dipole field within another, as the two are interacting:

$$H = -\frac{\mu_0}{4\pi}\frac{1}{r^3}[3(m_1 \cdot r)(m_2 \cdot r) - m_1 \cdot m_2] - \frac{2}{3}\mu_0 m_1 \cdot m_2 \delta^3(r) \quad (1.02)$$

To solve for the change in energy between the two states, we need to find the expectation value of H. To do this, we start with

$$E = \int \psi_0{}^* H \psi_0 d\tau \quad (1.03)$$

With ψ_0 being equal to

$$\psi_0 = (\pi a^3)^{-\frac{1}{2}} e^{-\frac{r}{a}} | s > \quad (1.04)$$

Solving equation (1.03) gives us

$$E = -\frac{2}{3}(\frac{\mu_0}{\pi a^3}) < m_1 \bullet m_2 > \quad (1.05)$$

The magnetic moment of the proton (m_1) and electron (m_2) are given by $m_1 = \gamma_p S_p$ and $m_2 = \gamma_e S_e$, respectively. Plugging those into equation (1.05) yields:

$$E = \frac{2}{3}(\frac{\mu_0}{\pi a^3})\gamma_e \gamma_p < S_e \bullet S_p > \quad (1.06)$$

Now we need to solve for $S_e \bullet S_p$

$$S_e \bullet S_P = \frac{1}{2}(J^2 - S_e{}^2 - S_p{}^2) \quad (1.07)$$

Both the electron and proton have spin-$\frac{1}{2}$, and the eigenvalues of $S_e{}^2$ and $S_p{}^2$ are $\frac{3}{4}h^2$, so

$$< S_e \bullet S_P > = \{\frac{1}{4}h^2\,(triplet),\ -\frac{3}{4}h^2\,(singlet) \quad (1.08)$$

Which leads to

$$E = \frac{2}{3}\frac{\mu_0 h^2}{\pi a^3}\gamma_e \gamma_p < \frac{1}{4}\,triplet,\ -\frac{3}{4}\,singlet \quad (1.09)$$

The words triplet and singlet refer to the spins of the particles. The singlet state is when the spins are antiparallel. The triplet state is when the spins are parallel, with $S = 1$, which allows for 3 possible values of the spin component ($M_s = -1, 0, +1$).

We can then find the change in energy

$$\Delta E_{hyd} = \frac{(\frac{\mu_0 h^2 e^2}{6\pi a^3}) g_e g_p}{m_e m_p} = 5.884 \times 10^{-6} eV \qquad (1.10)$$

With a numerical value for ΔE and h, we use $\nu = \frac{\Delta E}{h}$ to find the frequency, which is 1422.8 Mhz. The experimental value is 1420.4 MHz, with the 0.2% discrepancy being attributed to quantum electrodynamical corrections [6]. Then we can use the value of ν to find the wavelength using $\lambda = \frac{c}{\nu}$, which equals 21.07 cm. The spin-flip transition is technically a forbidden transition, and it only happens on the order of 10^7 years. However, there's so much neutral Hydrogen in the galaxy, roughly 90% of the interstellar medium, that we see it occur very often, allowing us to make these observations.

Galactic Geometry

The methods and geometry I will be using for creating the rotation curve are based on the work done in *Mapping the Spiral Structure of the Milky Way Galaxy at 21 cm Wavelength Using the SALSA Radio Telescope of Onsala Space Observatory* [7]. Calculating the rotational velocity relies on Newtonian mechanics. Orbital mechanics, such as in the case of our solar system, follow a Keplerian velocity curve, an example of this is seen in Figure 1.8 below.

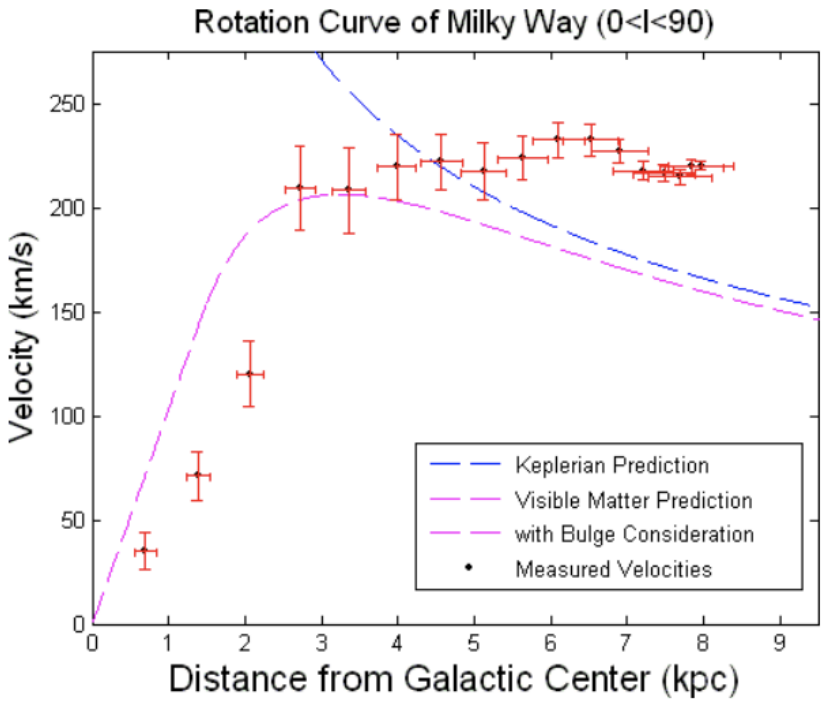


Figure 2.4 [8]: Rotation Curve of the Milky Way compared to a standard Keplerian curve and other predictions.

A Keplerian velocity curve functions as a plot of rotation speed versus distance from the center point. This is used in models of solar systems. It states that the speed of any orbiting object is inversely proportional to its distance, given by the equation:

$$v(r) = \sqrt{\frac{GM}{r}} \sim \frac{1}{\sqrt{r}}, \; r > r_0 \qquad (1.11)$$

This is Kepler's third law. It's a simple derivation from Newton's second law, which I'll present here. We start with Newton's second law of motion:

$$F_g = ma \qquad (1.12)$$

We also have the equation for the force of gravity:

$$F_g = \frac{G(M-m)}{r^2} \qquad (1.13)$$

Setting equations 1.12 and 1.13 equal to each other gives:

$$ma = \frac{G(M-m)}{r^2} \quad (1.14)$$

We then substitute a value for a:

$$m\frac{v^2}{r} = \frac{G(M-m)}{r^2} \quad (1.15)$$

Canceling out like terms leaves:

$$v^2 = \frac{GM}{r^2} \quad (1.16)$$

Taking the square root of v gives us Kepler's third law:

$$v = \sqrt{\frac{GM}{r}} \quad (1.17)$$

A galactic rotation curve is an upscaled version of the Keplerian velocity curve. Instead of being applied to a solar system, it is applied to model the movement of galaxies. Equation 1.11 shows the relation of orbital velocity if the total mass M of the system in enclosed within radius r_0. This is a standard Keplerian velocity curve, which is what the planets in our solar system follow. For bigger systems such as our galaxy, this simple model breaks down. As seen by the difference between the blue line and plotted marks in Figure 1.5, our galaxy doesn't have a rotation curve like this (due to uneven mass distribution) so a different model is required (dark matter also plays a part, which is explained on page 14). So we model the galaxy as a rotating symmetrical disk of various materials orbiting a center point instead. This assumption can be used as a placeholder until the data is used to determine the structure of the galaxy and the distribution of mass inside it. The Milky Way can be generalized to consist of two sections: The central bulge, which has a high luminosity and constant mass density, and the spiral arms and galactic disk, where the luminosity exponentially decreases with distance from the center. Finding the masses of these regions and the application of this to galactic geometry is detailed in the paper *The Hydrogen 21-cm Line and Its Applications to Radio Astrophysics* [8] and Figure 1.6 below:

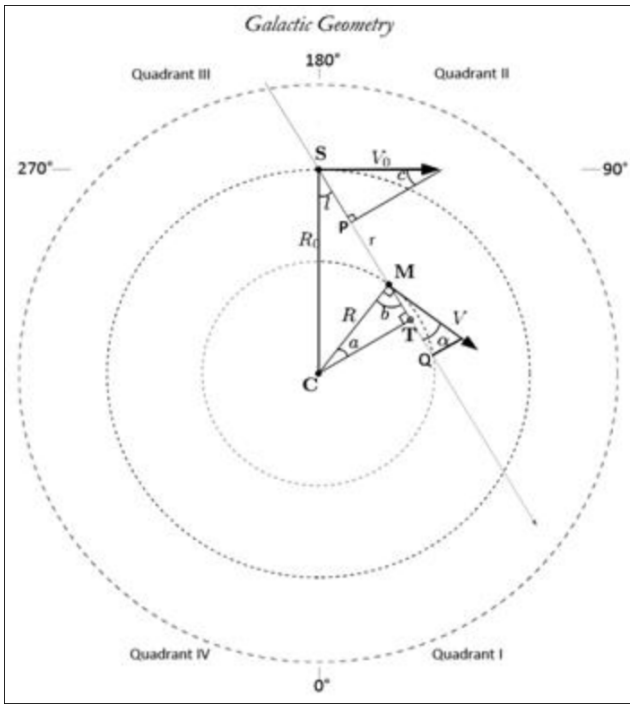


Figure 2.5 [7]: Simplified Geometry of the Milky Way Galaxy.

The Galactic Coordinate System

To accurately produce a map of the galaxy and a rotation curve, the coordinate system of the galaxy should be discussed. The galactic coordinate system used today was created by the International Astronomical Union in 1958. It standardized the use of Right Ascension and Declination, which corresponds to longitude and latitude on the celestial sphere, respectively. The celestial sphere is an imaginary sphere surrounding the earth that all the stars and constellations are plotted on, essentially a globe for astronomers. This is described in Figure 2.6.

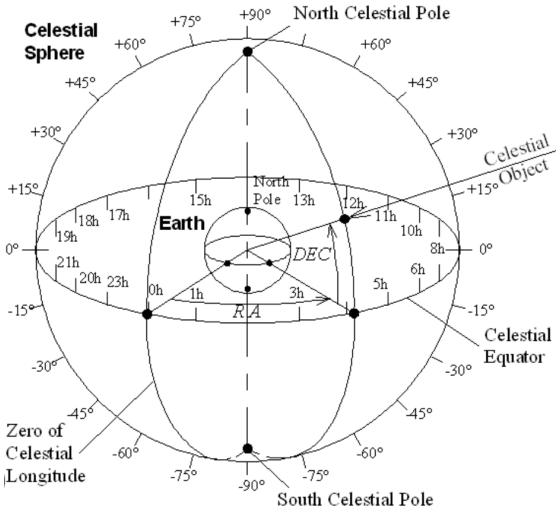


Figure 2.6 [14]: A visualization of the celestial sphere

When determining where to point the telescope, I use Stellarium to find the right ascension and declination, and then use that to find the Azimuth and Altitude coordinates, the second coordinate system used in this comp. Due to limitations from trees and buildings, the telescope can only view objects between 15 and 70 degrees longitude. While right ascension and declination are used in a spherical coordinate system across the entire sky, azimuth and altitude use a horizontal coordinate system. Measured from the observer, altitude is the angle from the horizon to the location of the object in the sky, and azimuth is its angle along the horizon. This is visualized below in Figure 2.7.

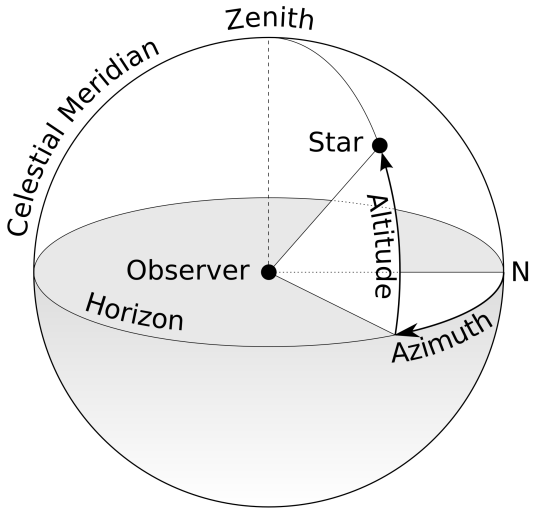


Figure 2.7 [15]: The horizontal coordinate system

The Role of Dark Matter

Determining what a galactic rotation curve should look like is difficult because it is affected by an unknown presence called Dark Matter. According to Kepler's 3rd Law, the rotational velocity of stars should decrease the further they are from the galactic center (I'm assuming a general Keplerian velocity curve for the moment despite knowing that is not the case). However, the curve remains flat and constant as distance increases, as seen in Figure 2.8. This should not happen unless there is a missing variable in the calculations. The presence of this missing variable was first noticed by Jan Oort in 1930 when observing the Milky Way, and by Fritz Zwicky in 1933 when observing the motion of galaxies in the nearby Coma cluster. Both Oort and Zwicky found that the motions of the stars within the galaxy and the motions of galaxies are too fast to keep any of them gravitationally bound to each other, so there must be missing matter in the halo regions surrounding the galaxies, keeping everything in place.

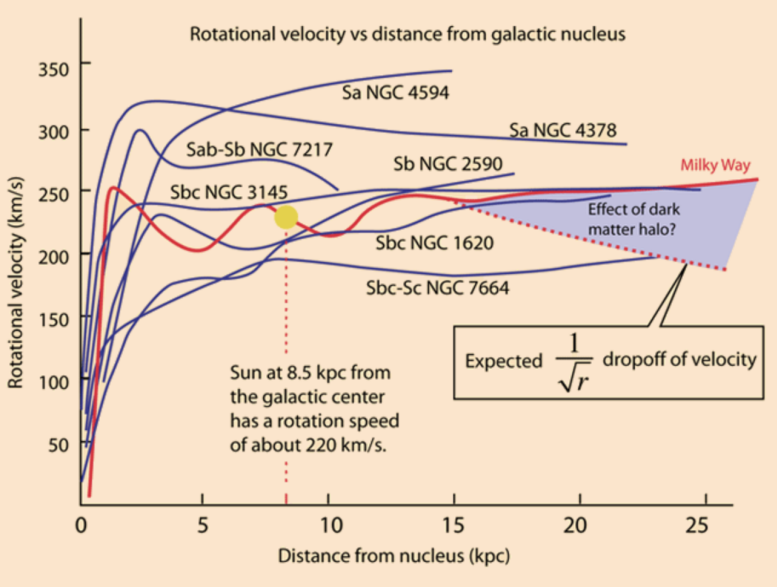


Figure 2.8 [11]: Rotation curves of multiple spiral galaxies & the Milky Way, with the dropoff predicted by a Keplerian velocity curve.

Methodology

Work had been done on the telescope in previous years to make sure it operates without any issues. As explained earlier, the telescope is a reflecting telescope that can move along the altitude and azimuth angles. The direction that the telescope is facing is controlled by PstRotator. Figure 3.1 below shows the control panel, with the up and down buttons moving the telescope along the altitude angles, and the left and right buttons moving it along the azimuth angle.

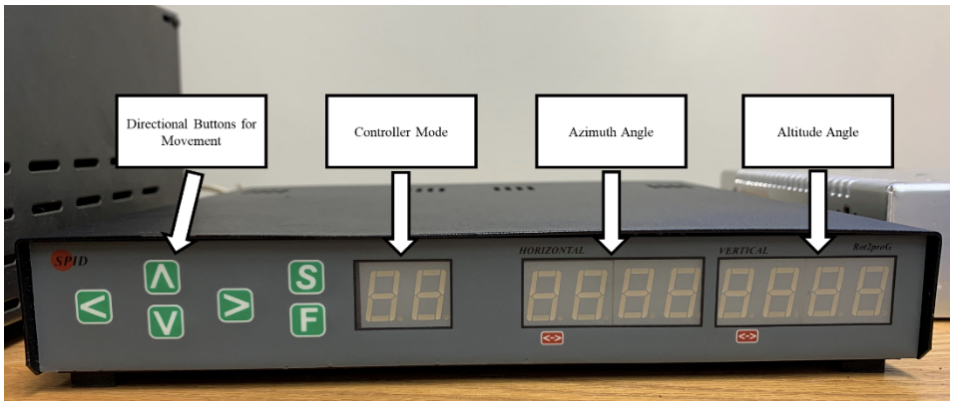


Figure 3.1: The PstRotator controller. Labels and photo were made by Ben Ramsey.

The 2-digit readout with the S and F keys are where the controller mode is set. Details on each control mode are in the user manual [9]. There is also a manual way to control the movement of the telescope with the computer mouse, but I have not looked into this because the digital way works fine. To determine the correct altitude and azimuth angle to take data, we use Stellarium, a program that shows the night sky in real-time, complete with nearly every cataloged deep sky object and coordinate data for these objects. It can also be adjusted to show the past and future placement of these objects. When adjusting the telescope, I choose a star or deep-sky object as close to the desired galactic longitude as possible (within 0.10°). I then write down the altitude and azimuth of that location and adjust the telescope as many degrees as I need until I achieve the same coordinates with PstRotator.

With the correct coordinates located, data collection can begin. SpectraCyber II, which is used to graph the data, is a very old application, with its current version only able to work in Windows Vista. Thus we use VirtualBox, an emulator to run Windows Vista on our Windows 10 operating system. SpectraCyber II is a relatively simple application and the most important to my work. The application can have two options for how it collects data, either through a spectral

sweep or a continuum sweep. Spectral sweeps take data at a single point at a time, which is what I use most often at this point in the comp. The graph in Figure 1.15 has the doppler shift of 1420.4 MHz on the x-axis and Voltage on the y-axis. A continuum sweep involves moving the telescope in an arc across the sky at a certain longitude, while it continuously takes data. I took a couple of those to test out the telescope after replacing the old LNA. I have been taking spectral sweeps of the sky at 5 degree intervals between 15 and 70 degrees galactic longitude, as that's where the sky isn't obstructed by buildings or trees.

Parameters used in SpectraCyber

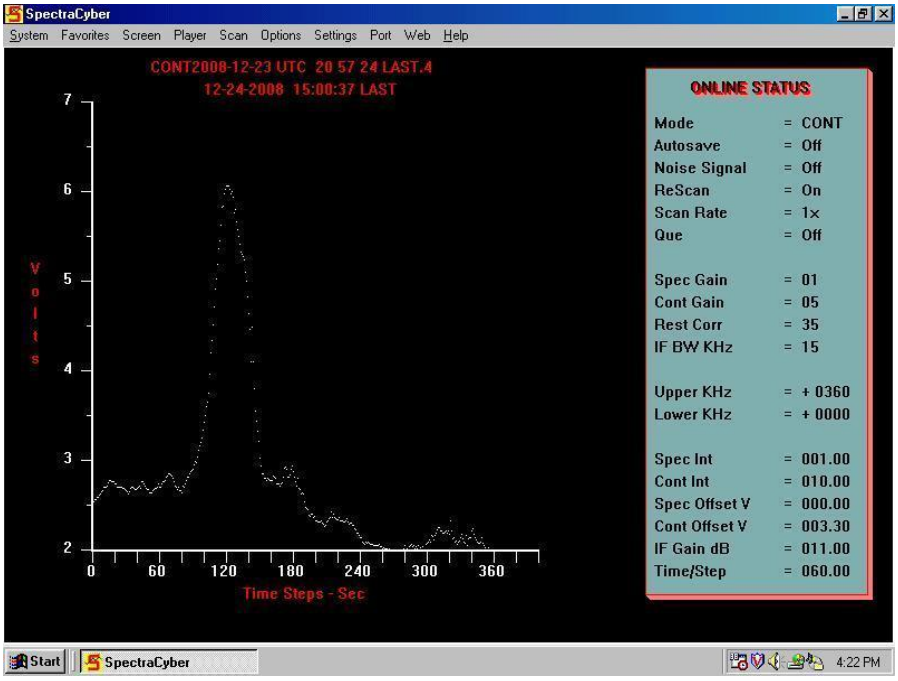


Figure 3.2: A graph of collected data for a continuum sweep. This is not my data, this is an example of what it should look like.

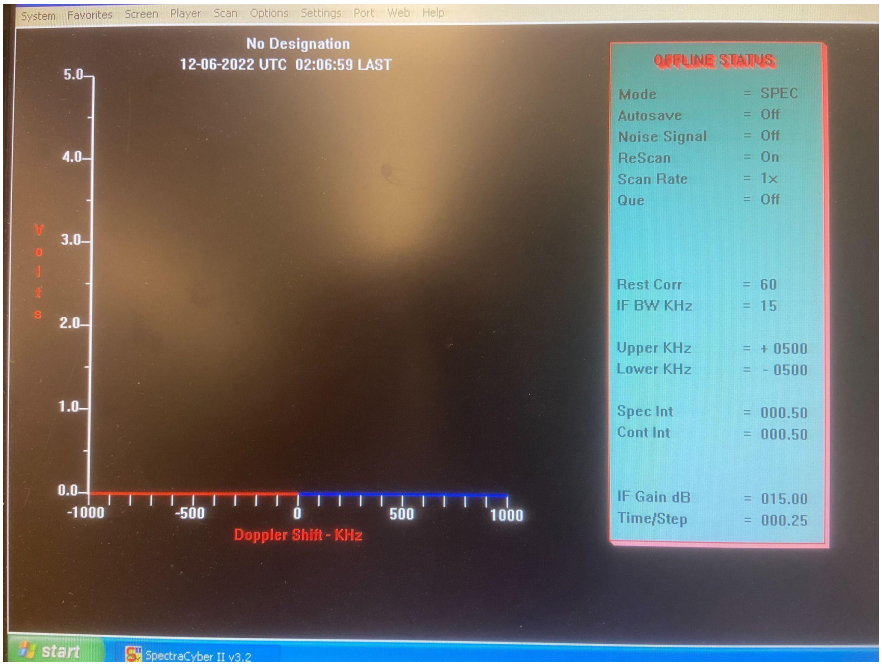


Figure 3.3: A photo of the SpectraCyber II interface in spectral sweep mode, with the parameters on the right

To make sure I get the correct data, the parameters need to be set in a certain way. Starting with the x-axis, which is the doppler shift of the observed cloud in KHz, the bounds need to be at -500 and 500. The gain (marked as IF Gain dB) can go up to a maximum of 25, but I usually set it at 15. I sometimes increase it to 20 to increase the intensity of the data if there is no clearly-defined peak in the data, there is too much random noise in the way, or if the signal does not appear strong enough. The difference between 15 and 20 can be very noticeable on the graphs. The time step is how often a data point is taken, in this case, it takes one data point per second.

Repairing the Telescope Motor

It became apparent that the problem with the blown fuses would only be fixed by ordering a new motor. Repairing the motor and the telescope took longer than expected due to many variables, much of which were out of my control. The motor arrived in late February, and I began work on fixing it by removing the old motor. This required me to remove the telescope

dish, which was aided by others in the physics department. This was done on February 24th. Since then, I have taken both the old and new motors apart to refit the wires into the new one.

Repairing the telescope dish

Throughout March, the telescope dish was leaning against the wall in the Carrden, in a position where I was sure that it couldn't fall over. However, my plans of reattaching the motor, conducting data tests with the feedhorn, and taking actual data for the end goal of calculating a rotation curve were all halted after a windstorm happened on the weekend of March 26th. The wind was very strong (even knocking out the power across Allegheny for around an hour). When I went to work the next day, I noticed that the telescope was no longer propped against the wall, and the steel brackets holding the feedhorn to the poles (and the poles as well) were warped, causing the feedhorn to be out of alignment, seen in Figure 4.3. The feedhorn is able to be adjusted by sliding it along the gaps in the L-brackets, as seen in Figure 4.4. These brackets need to be at exactly 90 degrees, which they were not. I used a vise in the machine shop to get the angles back to 90 degrees, or at least close enough, but they were still slanted in a way that made smooth adjustments impossible. The brackets are made out of steel, which limited the scale of adjustments I could make with the vise. I ended up having to go to the ALIC lab and get Professor Rich to help, which he successfully did.



Figure 4.2: The Radio Telescope after the storm



Figure 4.3: The Radio Telescope after I propped it back up



Figure 4.4: the L-brackets holding the feedhorn in place.

To realign the L-brackets, it required me to take the feedhorn apart, as the 4 struts were screwed in underneath the yellow-colored plate. Once they were realigned, I noticed an odd problem: The holes to fit the screws in were not big enough. Me and Dr. Willey used a machine drill to expand the width of each hole, which fixed the issue.I next had to fix the poles connecting the L-brackets to the dish. Being made out of Aluminium, these were easier to adjust in the vise. They also had to be at specific angles. The angle between the pole and the dish is at 121 degrees, and the angle between the pole and the brackets is at 119 degrees. With everything put back together in place, a new issue arose. The feedhorn was sliding along the brackets too easily, moving with no resistance. This should not happen. Me and Dr. Willey agreed that it is not an issue with the poles or the brackets, as those angle adjustments are correct. Dr Willey says that once the telescope is remounted, the problem should go away. As of the night of April 6th, I have thought that the lack of resistance for the feedhorn movement might be due to the washers that were originally there. When I took apart the feedhorn, there were originally 2 washers on

each screw, in between the pole connector and the bracket, these can partially be seen in Figures 1.4 and 4.4. The washers are currently in a labeled box on the desk in Room 111 in Carr Hall.

Rewiring the motor

Disconnecting the motor from the telescope, and disassembling the motor to access the inside did not take long at all. One issue is that the motor was made in Canada, so all the screws are in the metric system, and the department's wrenches are in the imperial system. This made disassembly into a game of trial and error with tool sizes. Another issue is the nature of rewiring the motor. There are eight wires (four that control the altitude, and four that control the azimuth), and there's no indication of which wire is which. The rotator manual gives vague instructions on the order of wire connection, so it required a fair bit of trial and error to determine which colored wire determines which effect.

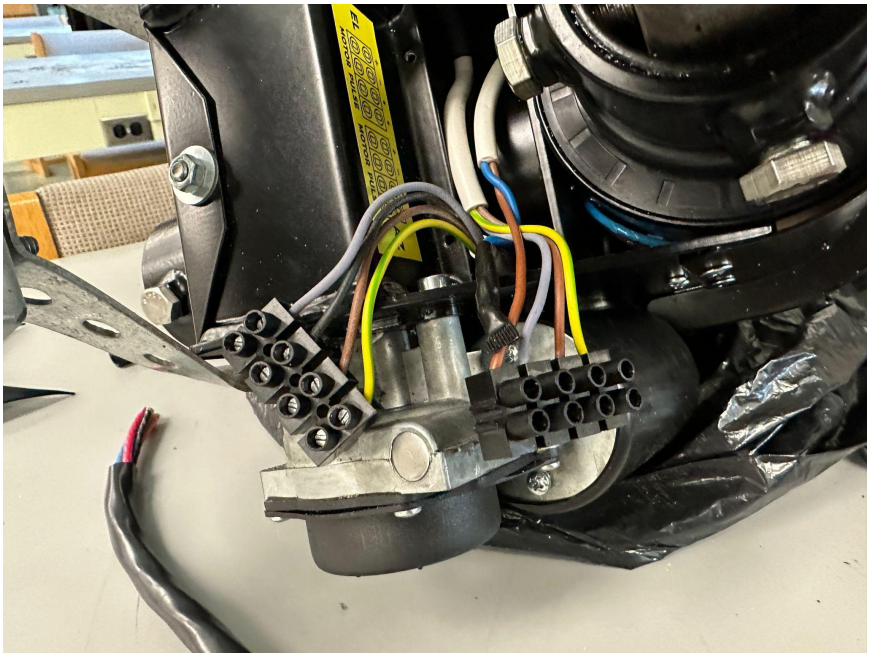


Figure 4.5: The eight wires that control the motor

In Figure 4.1, the four wires on the right control elevation, and the four on the left control the azimuth. I eventually found out the wire combination, at least for the elevation ones. The wire layout is seen in figure 4.6. Junction Box 1 is located on the pole that the telescope is mounted on, and Junction Box 2 is the lab. To make sure that these combinations were correct, I hooked

up the brown and gray wires (labeled positive and negative, respectively) to a voltmeter at 15 Volts that Dr. Willey provided, seen in Figure 4.7.

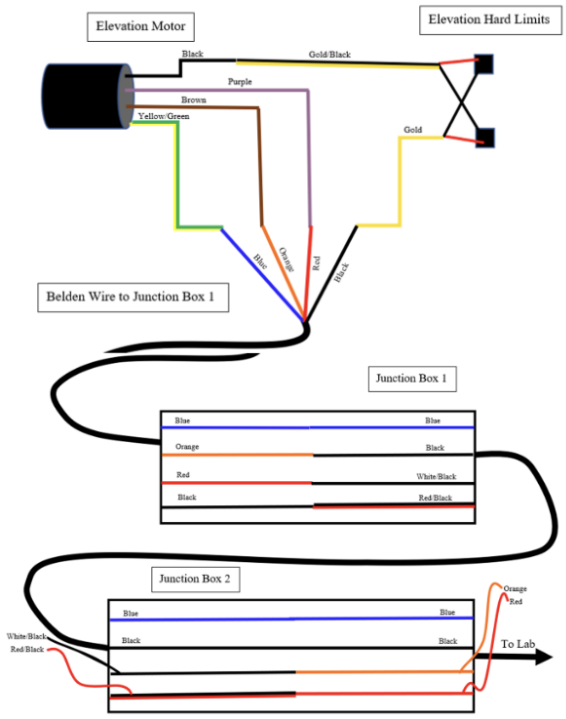


Figure 4.6 [12]: A diagram showing the wires connections between the motor and two junction boxes (not to scale).



Figure 4.7: The Voltmeter/Ammeter that Dr. Willey provided

Future Work

Unfortunately, this was as far as I was able to get with this project as of April 7th. I was hoping to do more work on the motor, but the windstorm pushed my schedule back with a static deadline. Whoever does their comp with the telescope next will have to do tests with the feedhorn at different lengths to see its effect on the signal strength in SpectraCyber, as well as finding the source of the periodic noise that continues to elude me. Recalibrating the telescope is also a top priority. This is done by attaching a compass to the base of the telescope, and changing the output on the compass (and ergo the telescope direction) until it matches with the output given by the azimuth controls.

Results

Spectral Sweeps

Since early October, I have been taking spectral sweeps of the area of the galaxy visible from the telescope from 15 to 70 degrees longitude, at 5 degree intervals. I have compiled

multiple sweeps at 15 and 20 degrees below in Figures 5.1-5.4. However, I do not have as much data as I would have liked.

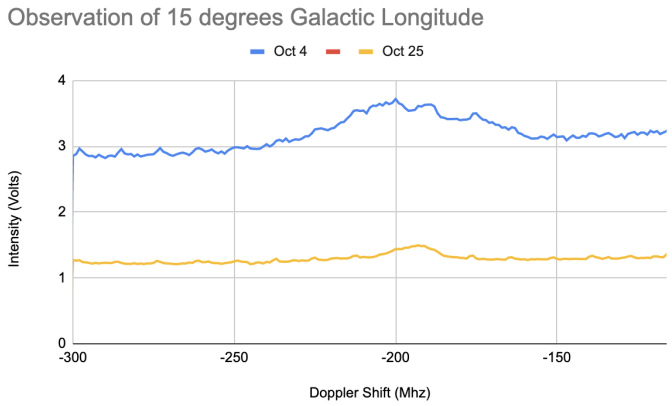
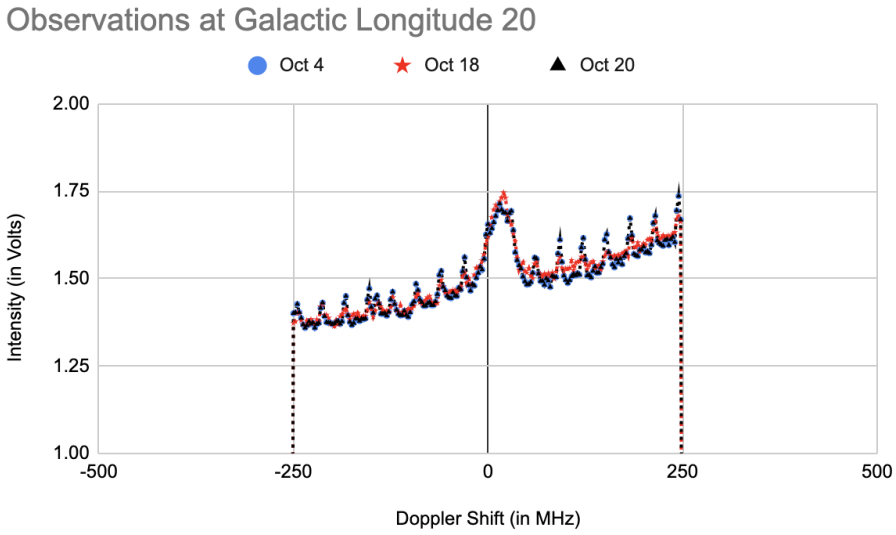


Figure 5.1: Plot of 2 spectral sweeps for 15 degrees galactic longitude.



=

Figure 5.2: Plot of 4 spectral sweeps for 20 degrees longitude

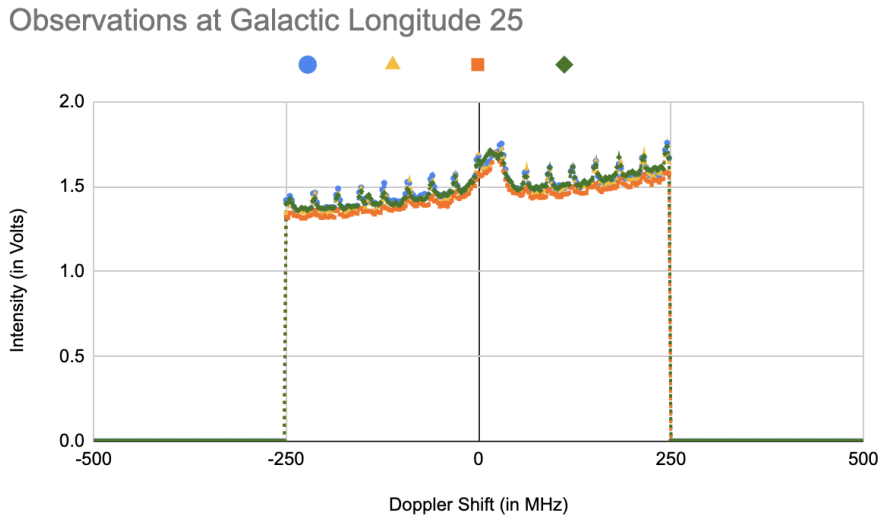


Figure 5.3: Plot of 4 spectral sweeps for 25 degrees longitude. The blue points are from October 4th, the rest are from October 20th.

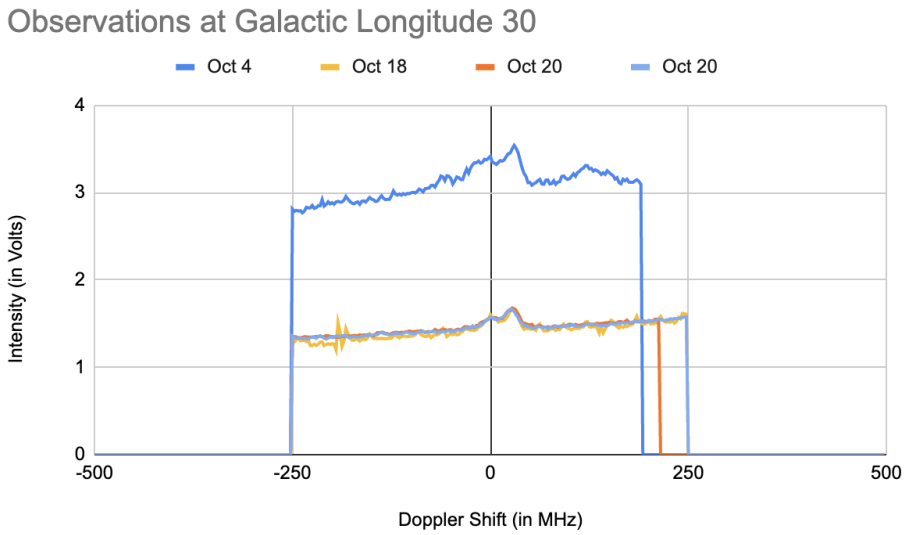


Figure 5.4: Plot of 4 spectral sweeps at 30 degrees longitude

The disparities between the majority of the plots and the measurements I took on October 4th are most likely due to a difference in Gain, as I would change the Gain and take a test measurement if the graph looked too flat or if the peak wasn't noticeable.

References

[1] National Radio Astronomy Observatory. (2022, Jan 20). *The History of Radio Astronomy*. https://public.nrao.edu/radio-astronomy/the-history-of-radio-astronomy/

[2] NASA. (n.d). *History of Radio Astronomy*. STEREO/WAVES. https://swaves.gsfc.nasa.gov/pdf_files/History%20of%20Radio%20Astronomy.pdf

[3] Storey, J. W. V. et al,. (n.d). *The 21cm Line of Atomic Hydrogen*. Retrieved from https://ugrad.phys.unsw.edu.au/physoc/radio/21cmhyd.pdf

[4] James Clerk Maxwell Foundation. (n.d). *Electromagnetic Theory.* https://clerkmaxwellfoundation.org/html/electromagnetic_theory.html

[5] Spectroscopy. (2007). The Electromagnetic Spectrum: A History. *Spectroscopy*, *22*(3).

[6] Griffiths, David J. (1980). Hyperfine splitting in the ground state of hydrogen. *Am. J. Physics, 50*(8), 698-708.

[7] Rashid Santo, T. Ashraf Uddin, S. (2013). Mapping the Spiral Structure of the Milky Way Galaxy at 21 cm Wavelength Using the SALSA Radio Telescope of Onsala Space Observatory. *International Journal of Astronomy.* doi:10.5923/j.astronomy.20130203.03

[8] Liu, L. Chronopoulos, C. The Hydrogen 21-cm Line and Its Applications to Radio Astrophysics. http://web.mit.edu/lululiu/Public/8.14/21cm/21cm.pdf

[9] Alfaspid. (n.d). *AlfaSpid Rotator and Controller Instruction Manual - WiMo*. Microsoft Word. https://www.wimo.com/media/manuals/SPID/25080_Rotor_Rotator_Manual.pdf

[10] *Electromagnetic Wave (Light Wave) vs. Mechanical Wave*. WebbTelescope.org. https://webbtelescope.org/contents/media/images/01F8GF5HE8JPQG4GTVFG6EPC23

[11] Nave, Carl R. (2017). Velocity Curves for Spiral Galaxies. *Hyperphysics.* Retrieved from http://hyperphysics.phy-astr.gsu.edu/hbase/Astro/velcurv.html

[12] Ramsey, B. (2019). *Exploring the Milky Way through 21 cm Radio Emission*

[13] Buchanan, B. (2023). *A Laser In Your Home? To Infinity And Beyond: MIMO, 6G, and Terahertz.* Retrieved from https://medium.com/asecuritysite-when-bob-met-alice/a-laser-in-your-home-to-infinity-and-beyond-mimo-6g-and-terahertz-4809f736c9ff

[14] *Astronomical Coordinate Systems.* Csun.edu. http://www.csun.edu/~boregan/astrolab/manual/unit012.htm

[15] *Celestial Navigation - The Celestial Sphere.* AstrolabeSailing.com https://astrolabesailing.com/2016/10/05/celestial-navigation-the-celestial-sphere/